Lattice fringe signatures of epitaxy on nanotubes

Jinfeng Wang and P. Fraundorf*
Physics & Astronomy and Center for Molecular Electronics, U. of Missouri-StL (63121), St. Louis, MO, USA

Yangchuan Xing
Chemical & Biological Engineering, U. Missouri-R (65409), Rolla, MO, USA

(Dated: March 11, 2006)

Carbon nanotubes are of potential interest as heterogeneous catalysis supports, in part because they offer a high surface area hexagonal array of carbon atoms for columnar or epitaxial attachment. Fringe visibility modeling of electron microscope lattice images allows one to investigate the relationship between individual nanoparticles and such nanotube supports. We show specifically how (111) columnar or epitaxial growth of FCC metal lattices, on carbon nanotubes viewed side-on, results in well-defined patterns of (111)-fringe orientations with respect to the tube axis. In the epitaxial case, the observations also provide information on chirality of the nanotube's outermost graphene sheet.

PACS numbers: 03.30.+p, 01.40.Gm, 01.55.+b

Contents

I. INTRODUCTION

Carbon nanotubes are of increasing interest for nanotechnology applications in general [1, 2]. They are also of interest as supports for heterogeneous catalysts [3, 4], for example in fuel cell applications [5]. Carbon nanotubes also have advantages for electron microscopy, because their near-cylindrical symmetry and propensity of lie perpendicular to the electron beam makes data acquisition and interpretation much simpler than for single crystal supports.

We show here that, with help from recent work on the theory of lattice fringe visibility [6, 7], that the crystallographic relationship between catalyst nanocrystals and their nanotube supports (Fig. 1) can sometimes be inferred from a single lattice fringe image. If the relationship is epitaxial, one might conversely decorate tubes in order to determine the chirality of their outer sheet. We illustrate the approach with a specific case: Growth of FCC metals on the top (0002) graphite (or graphene) surface of a carbon nanotube. The theory is easily extended to growth of other lattice types. Application to experimental images of Pt fuel cell catalyst crystals, on carbon nanotube supports, illustrates the strategy.

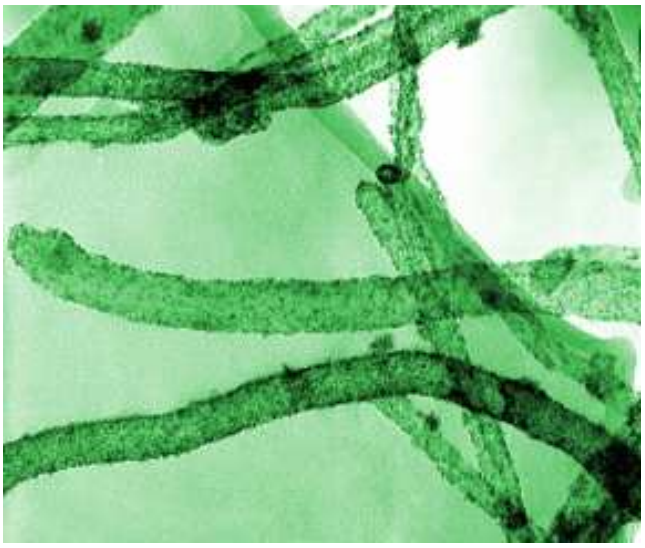

FIG. 1: Low magnification TEM image of Pt particles supported by carbon nanotubes [8].

II. THEORY

As aberration-correction makes it possible for electron microscope images to provide resolutions into the sub-Angstrom range, quantitative information contained in lattice fringes (Fig. 2) will become increasingly robust

*pfraundorf@umsl.edu

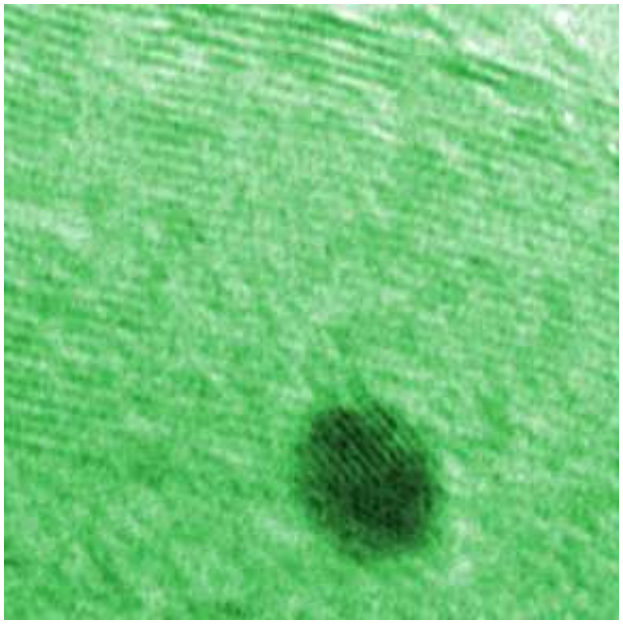

FIG. 2: High resolution image of a bicrystalline Pt nanoparticle on a carbon nanotube, half of which shows clear 0.26 nm (111) fringes.

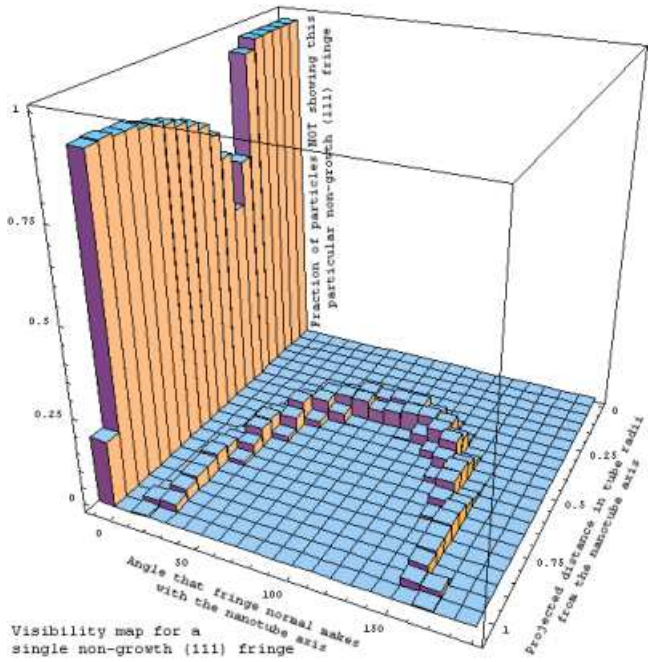

FIG. 3: Fraction of (111) columnar nanoparticles showing a given non-growth (111) fringe, as a function of azimuth angle of the fringe, and projected fractional radius, from the nanotube axis. This plot is for particles of 4.8 nm thickness. The histogram on the left roughly estimates the fraction of particles NOT showing this fringe.

[7]. In particular, on tilting away from the edge-on view of a lattice-plane in the transmission electron microscope (TEM), one encounters a range of incident electron angles (e.g. relative to lattice-plane parallel) within which the lattice plane's reciprocal lattice spots continue to intersect the Ewald sphere. Hence lattice fringes associated with those planes remain visible. The upper bound of this "visiblity band half-angle" (with the largest term first in the "thin specimen" limit) is

$$\alpha = \sin^{-1}\left[d\frac{\Gamma}{t} + \frac{\lambda}{2d}\left(1 - \left(d\frac{\Gamma}{t}\right)^2\right)\right]. \qquad (1)$$

Here d is the spacing of lattice planes, t is the crystal thickness, λ is the wavelength of the electrons, and Γ is a "visibility factor" on the order of 1 that empirically accounts for the signal-to-noise in the method used to detect fringes. The effective radius of the reciprocal lattice spot in this model (or excitation error s at which the fringe fades to background) is Γ/t.

We apply this theory to three types of relationship between supported FCC nanocrystals and underlying carbon and/or BN nanotubes: randomly oriented, (111) columnar, and (111) epitaxy. The objective is to illustrate the distribution of (111) lattice fringe orientations expected on a nanotube encountered by the electron beam "side on". The result is expected to be insensitive to slight deviations of the beam from perpendicularity to the tube axis.

A. Random orientations

For the random orientation case, we let each nanoparticle orient randomly to the electron beam. This might occur, for example, if the nanoparticles grow or accumulate with no regard to the underlying surface. Each nanoparticle has four sets of (111) lattice planes, in tetrahedral orientation to each other. From equation 1, the fringe will show up in the center of a 28[nm] diameter particle only when the electron beam is tilted by less than an α value of about 5 degrees out of that plane. For sufficiently thin particles, this result is relatively insensitive to the high energy of the electrons (e.g. 300[kV]) that the microscope is using.

Given that FCC crystals have four (111) planes which pairwise intersect down each of six $\langle 110 \rangle$ beam directions at an angle of $\theta_g = \cos^{-1}(1/3) \cong 70.5$ degrees, the fraction f_2 of particles showing cross-fringes at their center will be [7] about six times $2\alpha^2/(\pi \sin(\theta_g))$ or around 3%. The fraction f_1 of particles showing only 1 fringe at center will be $4\sin(\alpha) - 2f_2$ or around 29%. Hence about 68% of the particles will show no central fringes. Most importantly, as shown in the top central panel of 5, these probabilities will be independent of the projected position of each nanoparticle with respect to the nanotube's axis.

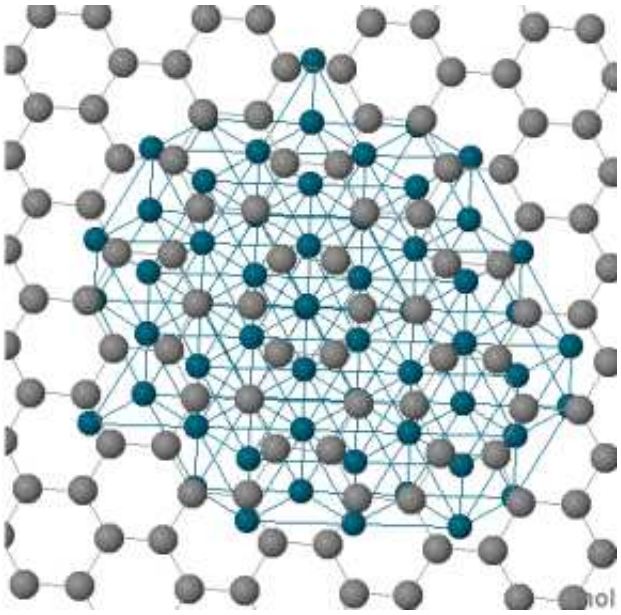

FIG. 4: Model of Pd (65 atoms) epitaxially grown on graphite (0002) or a graphene sheet surface.

B. Columnar growth down (111)

If the nanoparticles systematically grow upward from their substrate, along a column perpendicular to a (111) "growth plane" with no regard to the azimuthal orientation of the substrate beneath, we refer to this as (111) columnar growth. In this case the fringe abundances remain the same, but now those abundances depend on the projected position of the nanoparticle with respect to the nanotube axis.

In particular, the surface normal of a nanotube is tilted with respect to the incident electron beam by an angle θ equal to $\sin^{-1}(r/R)$, where r is the distance of the particle from the projected nanotube tube axis, and R is the nanotube radius. Consider now the unit normal to a lattice plane tilted up from the surface normal of the nanotube by θ_g, on an axis which makes an angle of ϕ with respect to the tube axis. If we let the electron beam direction define our viewer z-axis, and the projected tube-axis define the viewer x-axis, then that lattice plane normal in viewer coordinates has x-component $\cos(\phi)\sin(\theta_g)$, y-component $\cos(\theta_g)\sin(\theta) + \sin(\theta_g)\sin(\phi)\cos(\theta)$, and z-component $\cos(\theta_g)\cos(\theta) - \sin(\theta_g)\sin(\phi)\sin(\theta)$. As long as the normal to this plane deviates from perpendicularity to the beam by less than α, the fringe is visible and makes the angle predicted by it's x and y components.

Thus the growth (111) planes are only visible on top and bottom sides of the nanotube, when the beam direction is within three degrees of tangent to the nanotube surface. Also, as shown in Fig. 3, no particle-center (111) fringes are visible at all for projected locations on the nanotube within approximately one third of the tube radius from the center. The upper right corner of Fig. 5

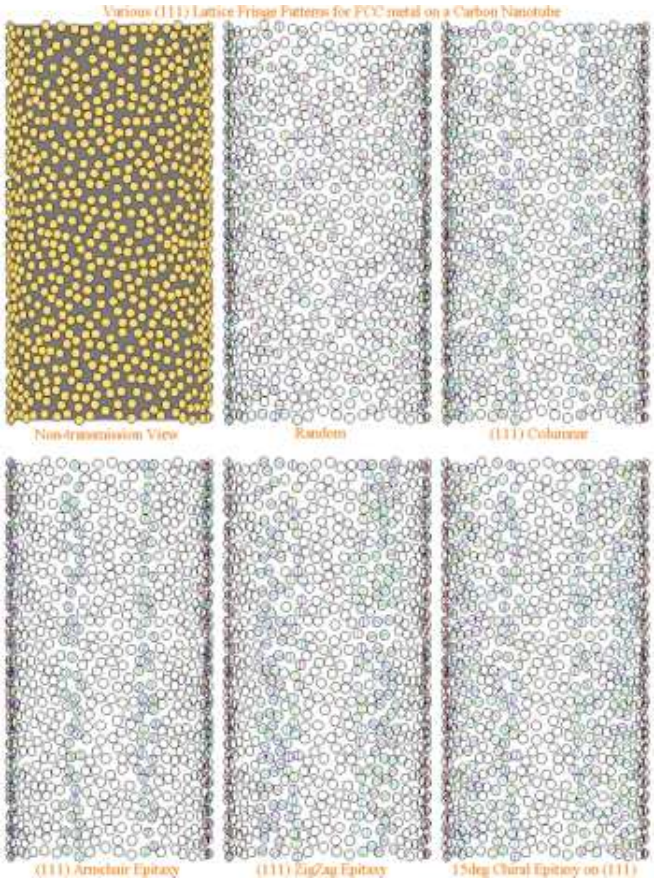

FIG. 5: Illustrated (111) fringe patterns expected for various 28A particles grown on a carbon nanotube, and observed with 300kV electrons.

shows that the resulting distribution of fringes is easily distinguishable from that expected for randomly-oriented particles.

C. Epitaxial growth on (111)

According to diffraction data in the literature [9], epitaxy of FCC Pd on single crystal graphite (0002) planes typically takes place with $(111)_{Pd}$ parallel to $(0002)_{graphite}$ in the growth direction, and $[112]_{Pd}$ parallel to $[01.0]_{graphene}$ in the plane of the substrate. This fully specifies the expected fringe distributions.

The bottom up view of such a 65 Pd-atom nanocrystal on graphene is shown in Fig. 4. Here for simplicity we've approximately positioned two of every three bottom-layer Pd atoms directly over a carbon atom, with the result that one of every three is over the center of a cyclohex graphene ring. The actual transitional alignment of the nanoparticle should have little effect on metal fringe visibility, provided that contrast from the underlying carbon does not obscure the metal lattice.

Because the Pd lattice azimuth is now fixed with respect to top graphene sheet of the underlying nanotube,

the fringe visible will be fully specified by the projected position for a given top sheet chirality. The result is illustrated at the bottom of Fig. 5 for armchair, zigzag, and "15 degree" chiral top-layer orientations, in sequence. As a fringe benefit, epitaxial "decoration" of carbon nanotubes might allow routine determination of top-layer tube chirality. Of course, as we discuss below, preparation of nanotube surfaces sufficiently clean and flat for epitaxial decoration may not be trivial.

III. EXPERIMENTAL TEST

In this experiment, we use a Philips EM430 supertwin TEM with point resolution near 0.2 nm to image Pt nanoparticles on nanotubes. In the images, we can find many Pt particle fringes. Pt is one of FCC elements [1]. Columnar growth along FCC (111) is, among other things, expected to result in (111) fringes parallel to the tube axis only along the tube edge, and at a projected distance from each tube edge of 1/3 the tube radius. When we magnify the fringe images, we find instead that projected Pt fringe angles are randomly distributed on the Carbon nanotube. So in this case nanoparticle growth is not along (111) columns.

IV. DISCUSSION

The foregoing illustrates the particular ease with which preferential crystallographic orientation can be detected in particles on nanotubes. However, preferential orientation on carbon nanotubes is complicated by two factors.

The first is surface integrity. For example in the experimental specimens above, it is easy to see that intact graphene layers only make it within a few atomic layers of the surface. This is likely due to an intentional roughening treatment designed to improve particle adhesion. Hence epitaxial growth would be impossible on these specimens, although columnar growth still conceivable.

The second complication is surface curvature. We're not aware of experimental data on the effects of graphene sheet curvature on epitaxy. For example, it may be possible only on larger diameter tubes. On the other hand, the technique of detecting epitaxy suggests that nanotubes substrates serve as an excellent candidates for experimental investigation of these sheet curvature effects.

Finally, we've worked through the mathematics here of one simple, and common, example of possible coherent relationships between carbon nanotubes and adhering particles. The methods used here should work seamlessly in other cases as well.

Acknowledgments

Thanks to MEMC Electronic Materials Company and Monsanto Corporation for regional facility support.

[1] M. S. Dresselhaus, G. Dresselhaus, and P. C. Eklund, *Science of Fullerenes and Carbon Nanotubes* (Academic Press, New York, 1996).
[2] H. Dai, Surface Science **500**, 218 (2002).
[3] P. N. Rylander, *Catalytic Hydrogenation in Organic Synthesis* (Academic Press, New York, London, 1979).
[4] J.M.Planeix, N.Coustel, B.Coq, V. Brotons, P.S.Kumbhar, R.Dutartre, P. Geneste, P. Bernier, and P. Ajayan, J. Am. Chem. Soc. **116**, 7935 (1994).
[5] W. Li, C. Liang, J. Qiu, W. Zhou, H. Han, Z. Wei, G. Sun, and Q. Xin, Carbon **40**, 787 (2002).
[6] W. Qin and P. Fraundorf, Ultramicroscopy **94**(3–4), 245 (2003).
[7] P. Fraundorf, W. Qin, P. Moeck, and E. Mandell, Journal of Applied Physics **98**, 114308 (2005).
[8] Y. Xing, Journal of Physical Chemistry B **108**, 19255 (2004).
[9] A.Humbert, M.Dayez, S. Granjeaud, P.Ricci, C.Chapon, and C. Henry, J. Vac. Sci. Technol.B **9(2)**, 804 (Mar/Apr 1991).